

Disruption causes in ASDEX Upgrade

G. Pautasso ⁽¹⁾, P.C. de Vries ⁽²⁾ and the ASDEX Upgrade team ⁽¹⁾

(1) Max-Planck-Institut für Plasmaphysik, 85748 Garching, Germany

(2) ITER Organization, Route de Vinon sur Verdon, 13115 St Paul Lez Durance, France

1. Introduction. Most of the existing tokamaks implement disruption protection measurements and can initiate a slow or fast (and mitigated) emergency shut-down; however no reliable disruption prediction system, which is portable to ITER, currently exists in present-day machines. A premise for avoiding or predicting unavoidable disruptions is knowing under which conditions they develop. In this paper, after a short discussion of the disruption rate during the ASDEX Upgrade (AUG) lifetime, the causes of the disruptions that occurred in 2013 (part of the 2012-2013 experimental campaign) are discussed. When possible, disruptions with similar causes are categorized according to the classification system used for JET [1]; in this process, attention has been paid to the chain of precursors preceding the instability. The plasma state directly before the thermal quench (TQ) is discussed. This comparison with JET will provide information on how universal these events are.

2. Disruption rate. The histogram in fig. 1 shows the percentage of discharges which disrupted with a plasma current (I_p) of at least 0.2 MA and 0.6 MA, relative to the number of discharges which reached a current of 0.2 MA, for each year of operation of AUG. This disruption rate has oscillated between 19 % and 61 % for the $I_p > 0.2$ MA set, and between 14 % and 32 % for the $I_p > 0.6$ MA set, over the years, without decreasing, and has been 40 % and 23 %, respectively, in average. These numbers contain also intentional disruptions; they are larger than those reported for JET, which show a learning curve decreasing the rate to values as low as 3-4 % for the carbon wall; nevertheless this rate increased again after the installation of the ITER-like Be/W wall to 10-20 %. The increase in the total disruption rate in 2007 in AUG also coincides with the completion of the transition from the carbon to the whole tungsten wall [2]. The apparent absence of a learning curve in fig. 1 has the following reasons. Firstly, AUG has been equipped since 2004 with a disruption mitigation system based on the locked mode (LM) detector and electromagnetic valves. Since 2011 also vertical displacement events (VDEs) are detected by the control system and mitigated. Damages have been caused by disruptions to in-vessel components in the past – mainly broken tiles and bent tile supports -, which have been progressively replaced by reinforced structures. No major disruption-induced damage has occurred in the last few years. Secondly, several experimental proposals continue to be aimed at studying reactor-relevant stability limits or high-risk scenarios and a large percentage of disruptions is intentional. Therefore, altogether there is not a big incentive to avoid disruptions in AUG.

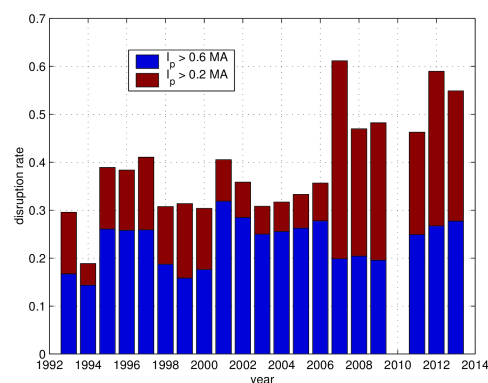


Fig. 1. Disruption rate during the AUG life time (right).

An analysis of the 2013 disruption database results in the following statistics:

- n. discharges with $I_p \geq 0.2$ MA (*): 847
- n. disruptions with $I_p(t_{\text{disr}}) \geq 0.2$ MA: 465, 55 % of (*)
- n. disruptions with $I_p(t_{\text{disr}}) \geq 0.6$ MA: 235, 28 % of (*)
- n. disruptions with $I_p(t_{\text{disr}}) \geq 0.6$ MA analysed (**): 196
- n. “intentional” disruptions with $I_p(t_{\text{disr}}) \geq 0.6$ MA: 50, 26 % of (**)
- n. disruptions in “high risk” discharges with $I_p(t_{\text{disr}}) \geq 0.6$ MA: 46, 23 % of (**)

The non-intentional disruptions amount to 74 % of the total occurrence in 2013; the label “high risk” is assigned to experiments at $q_{95} \sim 3$ (ITER baseline scenarios, among others), at low density with RMPs and on partial divertor detachment with N_2 puff and high input power.

3. Instability and disruption precursors. Following the method outlined in [1], the time evolution of several plasma and machine parameters during the pre-disruption phase of the 2013 disruptions have been analysed. Several physics instabilities reported in Table I (a) of [1] are also usual disruption precursors in AUG. We list here the common ones, without discussing in detail (due to lack of space) why others are omitted: Greenwald limit, high density (close to Greenwald), low density (and low safety factor, q_{95}), radiation collapse (cold edge and internal inductance, li , peaking), radiation peaking, MARFE, H-to-L back transition (common to most disruptions), neoclassical tearing mode (NTM), MHD other than NTM, LM, VDE, and $q_{95} \sim 3$ (new on AUG). Disruptions preceded by similar sequences of precursors are grouped in the same class (see sec.4). The technical problems hampering the AUG operation have not been analysed in detail; however they are believed to have a small impact on the rate of disruption occurrence.

4. Disruption classes. The different classes listed in Table II of [1] are found to be useful to cluster the AUG disruptions and are discussed, from the AUG point of view, in this section. In addition, their location on the $li(q_{95})$ diagram is shown in Fig. 2. The upper boundary of Fig. 2 is typically populated by cases of cooling of the plasma edge and contraction of the current profile; the contribution to the lower boundary comes from current rise instabilities and hollow or flat current profiles due to impurity accumulation. A third, here-invisible – since avoided – boundary is a vertical line at $q_{95} \sim 2$. The upper and lower boundaries for AUG and JET coincide (not shown), indicating common instability mechanisms in their proximity and thus justifying the chosen representation.

Greenwald limit (JET: GWL). The L- and H-mode density limits (DLs) have been investigated on AUG in 2013. The DL is intentionally induced by continuous strong gas puffing of the main plasma species until disruption. The chains of events preceding DL disruptions have been described in several publications ([3] and references within); the physical mechanisms leading from one event to the other have been identified and, even if not in detail, mostly understood. Cases in which the plasma was fueled and the gas flow was too large, because erroneously programmed, were not found in the set of discharges considered.

Low density EF mode (JET: EFM). Studies of error fields have been carried out in the last 2 years by generating an $n=1$ radial magnetic field, resonant on the $q=2$, with the recent installed RMP coils in low density and low q_{95} plasmas. These disruptions are *intentional* (AUG:EFX). *Unintentional* disruptions, occurring at low density, with or without RMPs and with $q_{95} > 3$, are indicated with LON (low density) in Fig. 2 (c). The EFX and LON classes are localized on the upper $li(q_{95})$ boundary.

Too strong core radiation (JET: RPK). Impurity accumulation is common in AUG under certain plasma conditions: insufficient heating of the plasma core, low density, absence of gas puff and ELM free phases. Impurity accumulation occurs over the time scale of hundred ms and it is easily detectable by the bolometers. A controlled pulse termination (used in the past but not in 2013) can be initiated to avoid the thermal collapse of the whole plasma, leading to disruptions. A similar disruption class appeared at JET after the introduction of the W divertor.

Cold edge (CE). Plasmas which develop a cold edge and a peaked current profile, end on the upper boundary of the $li(q_{95})$ diagram. Cases, which could not find another affiliation, are gathered in this group.

Neoclassical tearing mode (NTM). NTMs are very often present during the H mode phase of AUG discharges and can degrade the confinement. In order to induce a disruption, a stationary NTM must evolve into one or more growing modes, usually with an harmonic structure different from the stationary. The *intentional* high beta discharges (DAV in Fig. 2 (a)) used for the so-called “disruption avoidance experiments” are an example of this class.

Additional few and clear cases of short-lived NTMs, terminating a pulse, have been included in a more extensive group of disruptions caused by the growth of tearing modes (MOD). These disruptions are scattered on the central part of the $li(q_{95})$ diagram, and the identification of their destabilizing mechanisms requires further analysis.

Current ramp-up (IPR). These disruptions occur towards the end of the ramp-up phase or beginning of flat-top, mostly when auxiliary heating has not yet been applied. This group comprises discharges with li close to the upper boundary of the $li(q_{95})$ stability diagram and others close to the lower boundary (see fig. 2 (c)).

Vertical stability control problem (VSC). AUG operated several years (the first decade) with only sporadic accidental VDEs. They became more and more frequent in the last decade of operation for the following reasons: a part of the VDEs could be attributed to a pre-programmed equilibrium which had, among others, a large vertical growth rate and could not be easily stabilized by the control system; the remaining cases are mostly loss of vertical stability due to current spikes induced by MHD activity. Since these last cases became more and more frequent as the fraction of tungsten increased as PFC material, an algorithm for the detection and mitigation of VDE was implemented in the control system in 2011. The majority of mitigated shut-downs are initiated by a loss of vertical control following current spikes in 2013. Only the VDE without 3-D MHD precursors are assigned to this group.

Shape control problem. This can occur when a new equilibrium configuration is developed. Since it typically leads to the loss of vertical stability, these cases are classified as VSC.

Auxiliary power shut-down (ASD). NBI power turned off during phases of high plasma density and impurity content cause a disruption. This can happen more or less accidentally during the flat-top or the ramp-down, respectively.

Fast emergency shut-down (FSD). The AUG protection system foresees a fast ramp down (PST = pulse stop) of all coil currents, when an emergency controlled shut-down is not possible for technical reasons. Under these circumstances, which are rare, the uncontrolled plasma is terminated with MGI.

Other classes of disruptions comprise: intentional MGI experiments; mitigation erroneously triggered by a LM signal crossing the protection threshold, without the presence of a LM; disruptions at $q_{95} \sim 3$, and after current spikes (not preceded by a mode), causing loss of vertical stability; impurity control problems (**IMP**), after the use of impurity puffing for the control of the power onto the divertor.

Table 1 summarizes and compares the rate of occurrence of disruptions, subdivided by class, in AUG and in JET. The most evident difference is the smaller percentage of disruptions during impurity accumulation in AUG, which reflects the capability of this device to centrally heat the plasma with ECRH in most of the experimental scenarios.

5. Terminal precursors. Disruptions in AUG are always preceded by a 3-D MHD instability, typically rotating or locked tearing modes (since kinks are rarely observed to terminate a discharge) or by a VDE. Finding measurable properties of these instabilities, which can be used to predict an imminent disruption, has been the purpose of the work presented in [4]. This analysis concentrated on the LM amplitude; nevertheless, AUG disruptions are not always preceded by a detectable LM (that is a LM amplitude which is larger than the excursions of the LM signal due to the spurious pick up of radial magnetic field from coil currents). Two reasons behind this fact have been already reported in [4]: the LM amplitude preceding the TQ onset is found to scale linearly with li and with $1/q_{95}$. A large percentage of plasmas disrupt during impurity accumulation in AUG with the W wall and when li is small; during the ramp-up and -down, q_{95} is larger than in the flat-top; in all these cases the LM amplitude is found to be small. A second reason is that often a rotating mode is seen to cause a partial or global TQ and therefore it is the still-rotating-mode amplitude which should be measured and used as predictor. Some of the terms in the sequence “mode growing, mode slowing down, LM, current spike, TQ, vertical instability” are always present before a disruption. Nevertheless a mode can grow “locked” without being detected as an oscillation by the Mirnov coils; a still-rotating mode can cause a current spike and initiate a TQ or VD; a current spike does not have to cause a global TQ, particularly during impurity accumulation; the first part of the sequence can repeat itself several times (typical of the W machine) leading eventually to the loss of vertical stability.

6. Summary. The classification developed for JET turned out to be very useful for a preliminary clustering of the AUG disruptions. The same classes of disruptions are found in both devices; however the likelihood of each class is different, reflecting the diverse heating systems, competences and experimental programme. This work provides a framework for further analysis of these events separately, on each machine, and then jointly. The ultimate aim of this common analysis is the formulation of universal criteria for disruption avoidance and prediction.

Acknowledgement. The first author thanks E. Wolfrum, one of the AUG experimental leaders, for constructive input. The views and opinions expressed herein do not necessarily reflect those of the ITER Organization. This project has received funding from the Euratom research and training programme 2014-2018.

- [1] P.C. de Vries et al., *Physics of Plasma* 21, 056101 (2014)
 [2] R. Neu et al., *Plasma Science, IEEE Transactions on* 42, 3 (2014), 552-562
 [3] M. Bernert et al., “*The H-mode density limit at the ASDEX Upgrade tokamak*”, this conference
 [4] P.C. de Vries et al., “*MHD perturbation amplitudes required to trigger disruptions*”, this conference
 [5] P.C. de Vries et al., *Nuclear Fusion* 51, 053018 (2011)

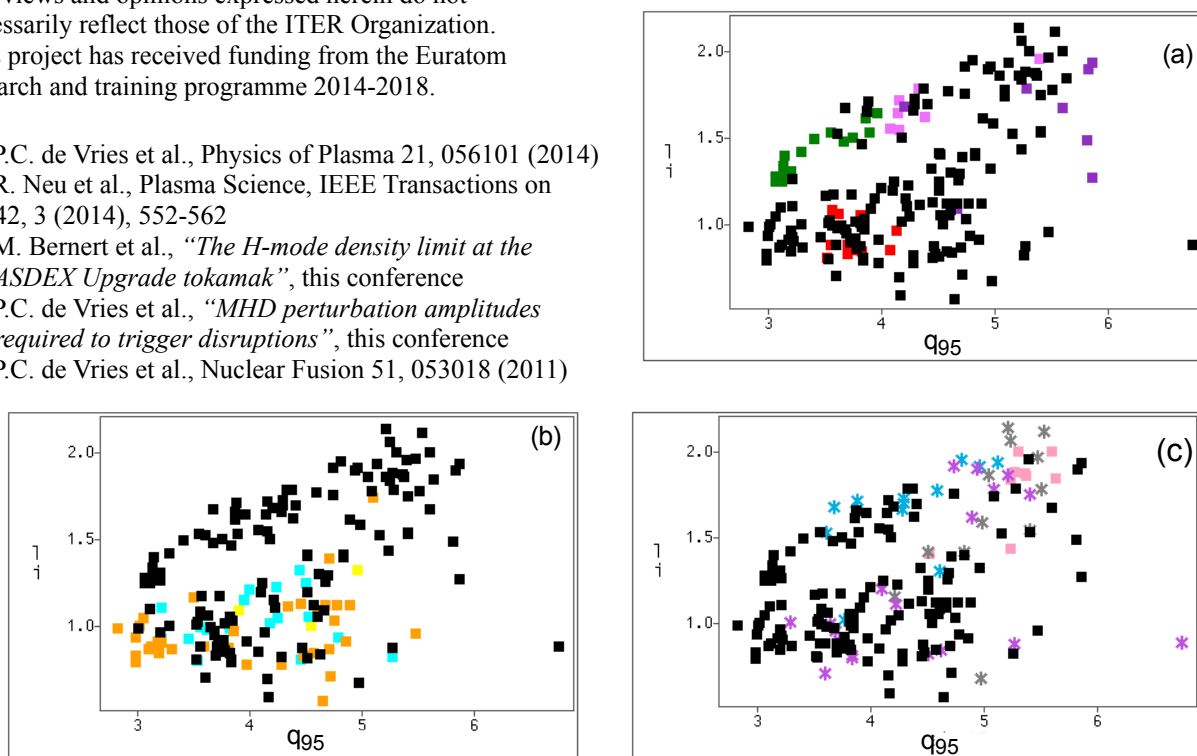


Fig. 2 (a) - (c). Clustering of AUG disruptions (selected classes) on the $li(q_{95})$ stability diagram. Black symbols represent not selected discharges.

Where in Fig. 2	Symbol Fig. 2	AUG class	AUG discr. rate 2013	JET class	JET 2000 - 2009 [5]	ITER ILW 2011 - 2012 [1]
(a)	■	GWL (L mode)	4.1 %	Included in NC		
(a)	■	GWL (H mode)	4.6 %	GWL	2.4 %	0.0 %
(a)	■	EFX	9.7 %	/	/	/
(a)	■	DAV	6.1 %	/	/	/
(b)	■	RPK	17.9 %	RPK	0.0 %	47.6 %
(b)	■	IMC	1.5 %	IMC	18.7 %	16.8 %
(b)	■	MOD	9.7 %	NTM	8.2 %	5.1 %
(c)	*	ASD	7.7 %	ASD	10.0 %	0.7 %
(c)	*	IPR	10.2 %	IPR	5.9 %	1.1 %
(c)	*	LON	6.6 %	EFM	5.6 %	8.4 %
(c)	■	CE	5.6 %	Included in NC?		
not shown		VS + SC	6.6 %	VS	4.6 %	0.6 %
not shown				SC	6.0 %	1.1 %
not shown		others	~ 10 %	NC	15.6 %	10.3 %

Table 1. Comparison between AUG and JET of the percentage of disruptions occurred in each class.